The Astrophysical Journal, 654:L25–L28, 2007 January 1
© 2007. The American Astronomical Society. All rights reserved. Printed in U.S.A.

MULTICOLOR SHALLOW DECAY AND CHROMATIC BREAKS IN THE GRB 050319 OPTICAL AFTERGLOW

K. Y. Huang,[1] Y. Urata,[2,3] P. H. Kuo,[1] W. H. Ip,[1] K. Ioka,[4] T. Aoki,[5] C. W. Chen,[1] W. P. Chen,[1] M. Isogai,[5] H. C. Lin,[1] K. Makishima,[3,6] H. Mito,[5] T. Miyata,[5] Y. Nakada,[5] S. Nishiura,[7] K. Onda,[2] Y. Qiu,[8] T. Soyano,[5] T. Tamagawa,[3] K. Tarusawa,[5] M. Tashiro,[2] and T. Yoshioka[9]

Received 2006 June 12; accepted 2006 November 9; published 2006 December 7

ABSTRACT

Multiwavelength observations of the optical afterglow of GRB 050319 were performed from 1.31 to 9.92 hr after the burst. Our *R*-band light curves, combined with other published data, can be described by the smooth broken power-law function, with $\alpha_1 = -0.84 \pm 0.02$ to $\alpha_2 = -0.48 \pm 0.03$, 0.04 days after the gamma-ray burst. The optical light curves are characterized by shallow decays—as was also observed in the X-rays—which may have a similar origin, related to energy injection. However, our observations indicate that there is still a puzzle concerning the chromatic breaks in the *R*-band light curve (at 0.04 days) and the X-ray light curve (at 0.004 days) that remains to be solved.

Subject heading: gamma rays: bursts

On-line material: machine-readable table

1. INTRODUCTION

The gamma-ray burst (GRB) afterglow as perceived in the X-ray, optical, and radio wavelengths is now understood to be the result of the collision between relativistic ejecta from the gamma-ray bursts and the interstellar medium (ISM). A comparison of afterglow light curves obtained at different wavelengths gives us important information about the surrounding ISM environment and the interaction processes. Such analyses can also provide essential input for theoretical models. Recently, the pace of this type of activity has quickened significantly, stimulated by the capabilities of the quick response and accurate localization of GRBs by the *Swift* satellite (Gehrels et al. 2004). This has meant that the number of GRB optical afterglow detections in the first several hours after a GRB by ground-based telescopes has recently increased significantly. It is interesting to note that the observations by *Swift* of the early X-ray emissions from a number of GRBs reveal a canonical behavior. The X-ray light curves can be divided into three distinct power-law segments (Nousek et al. 2006). Some X-ray and optical observations show that the evolution of both light curves changes at the same time (Blustin et al. 2006; Rykoff et al. 2006); however, chromatic breaks were also found in some cases (Fan & Piran 2006; Panaitescu et al. 2006). The nature of the afterglow early breaks in the light curves is thus uncertain. A detailed comparison of changes in the evolution of the optical, radio, and X-ray light curves should therefore be very interesting. This kind of physical study demands both a well-coordinated observational program and careful data analysis. We use GRB 050319, which has comprehensive observational coverage in both the X-ray and optical wavelengths and may be used as just such an example.

GRB 050319 was detected by the Burst Alert Telescope (BAT) on board the *Swift* satellite on 2005 March 19 at 09:31:18.44 UT (Krimm et al. 2005). However, a reanalysis of the BAT data showed two flares, indicating that GRB 050319 had already started 137 s before the trigger. The 15–350 keV fluence for the entire burst duration of $T_{90} = 149.6 \pm 0.7$ s has been estimated to be 1.6×10^{-6} ergs cm^{-2}. The X-ray emission of GRB 050319 after the burst was monitored by the *Swift* X-Ray Telescope (XRT) from 225 s to 28 days.[10] Two breaks in the emission curves were found (Cusumano et al. 2006). The initial sharp decline can be described by a power law with an index of $\alpha_1 = -5.53 \pm 0.67$ to be followed by $\alpha_2 = -0.54 \pm 0.04$ about 0.004 days after the burst. The unusually flat decline in the second part might have been caused by continuous energy injection. At about 0.313 days after the burst, the power-law index changed to $\alpha_3 = -1.14 \pm 0.2$, which can be readily explained as a jet break or a reduction in the energy injection (Cusumano et al. 2006; Zhang et al. 2006).

The early optical afterglow emission at 230 s was observed by the UV/Optical Telescope (UVOT) on *Swift* (Mason et al. 2006) and by two ground-based robotic telescopes, ROTSE-III (Robotic Optical Transient Search Experiment; Quimby et al. 2006) and RAPTOR (Rapid Telescopes for Optical Response; Woźniak et al. 2005). The best single–power-law fit of unfiltered data from ROTSE-III and RAPTOR indicates that $\alpha = -0.854 \pm 0.014$. A number of optical observatories have joined the follow-up observations (Yoshioka et al. 2005; Torii 2005; Sharapov et al. 2005a, 2005b; George et al. 2006; Misra et al. 2005; Kiziloglu et al. 2005; Greco et al. 2005). The spectral measurements of the afterglow by the Nordic Optical Telescope (NOT) indicate the redshift $z = 3.24$ of this event (Jakobsson et al. 2006).

2. OBSERVATIONS AND ANALYSIS

After receiving the GRB alert message from *Swift* and after the afterglow position was reported by Quimby et al. (2006), the Target-of-Opportunity procedures of the East-Asia GRB

[1] Institute of Astronomy, National Central University, Chung-Li, Taiwan; d919003@astro.ncu.edu.tw.
[2] Department of Physics, Saitama University, Shimo-Okubo, Sakura, Saitama, Japan.
[3] RIKEN, Hirosawa, Wako, Saitama, Japan.
[4] Department of Physics, Kyoto University, Kyoto, Japan.
[5] Kiso Observatory, Institute of Astronomy, University of Tokyo, Mitakemura, Kiso-gun, Nagano, Japan.
[6] Department of Physics, University of Tokyo, Hongo, Bunkyo-ku, Tokyo, Japan.
[7] Department of Astronomy and Earth Sciences, Tokyo Gakugei University, Koganei, Tokyo, Japan.
[8] National Astronomical Observatories, Chinese Academy of Sciences, Beijing, China.
[9] Department of Physics, Nagoya University, Furo-cho, Chikusa, Nagoya, Aichi, Japan.

[10] The burst time in the article is 09:29:01.44 UT, 137 s before the BAT trigger.

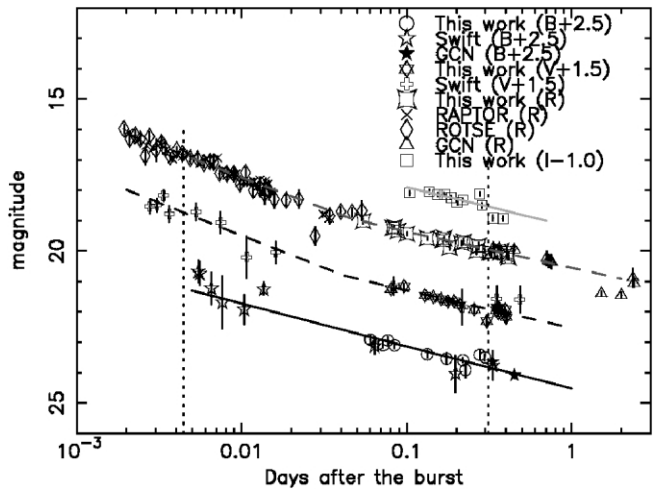

FIG. 1.—Optical light curves of GRB 050319. The solid lines present the best fit by the single power-law model ($F \propto t^{\alpha}$) for the *B* band ($\alpha = -0.56 \pm 0.06$) and the *I* band ($\alpha = -0.52 \pm 0.15$). The dashed line indicates the best fit by the smooth broken power law (eq. [1]) with the *V* band ($\alpha_1 = -0.87 \pm 0.21$, $\alpha_2 = -0.49 \pm 0.05$, $t_b = 0.042 \pm 0.058$ days) and the *R* band ($\alpha_1 = -0.84 \pm 0.02$, $\alpha_2 = -0.48 \pm 0.03$, $t_b = 0.046 \pm 0.008$ days). The dotted lines represent the break times of X-ray afterglows 0.004 and 0.31 days after the burst. The two breaks were not found in X-ray observations, but a mild break seems to exist in the *V*- and *R*-band light curves.

Follow-up Observation Network (EAFON; Urata et al. 2005) were immediately carried out. A series of multiband follow-up observations were successfully performed by the 1.05 m Schmidt telescope of the Kiso Observatory in Japan and the Lulin One-meter Telescope (LOT) in Taiwan. Photometric *B* and *R* images were obtained at the Kiso site with a 2K × 2K CCD camera (Urata et al. 2005) between 0.055 and 0.326 days after the burst. A number of parallel *B*, *V*, *R*, and *I* images were obtained by LOT with a PI1300 CCD camera (Kinoshita et al. 2005) from 0.080 to 0.413 days after the burst.

The standard routine included bias subtraction and dark subtraction; flat-field corrections were employed with the appropriate calibration data needed to process the data using IRAF. The signal-to-noise ratio was improved by combing the LOT *B*-band data with median filtering. The DAOPHOT package (Stetson 1987) was then used to perform point-spread function (PSF) fitting for the GRB images. Four field stars were used to create a PSF model that was applied to the optical afterglow of each GRB image. For absolute photometric calibration, we used calibrated data of the GRB field obtained by Henden (2005). The photometric error and the systematic calibration error were included in the magnitude error estimation.[11]

3. RESULTS

3.1. *Light Curve*

Figure 1 shows the multiband light curves of the GRB 050319 afterglow. Besides our *B*-, *V*-, *R*-, and *I*-band data (Table 1), we also included the *R*-band measurements from ROTSE-III (Quimby et al. 2006), RAPTOR (Woźniak et al. 2005), and several GRB Coordinates Network (GCN) reports (Greco et al. 2005; Kiziloglu et al. 2005; Misra et al. 2005; Sharapov et al. 2005a, 2005b). In addition, we also made use of several *B*- and *V*-band measurements taken with the *Swift* UVOT (Mason et al. 2006). The GCN *R*-band points were recalibrated using the GRB 050319 field stars reported by Henden (2005), so they could be plotted on the same magnitude scale. The magnitude differences between the photometric field stars in Henden (2005) and the USNO-A2.0 and USNO-B1.0 stars are +0.18 and −0.22 mag, respectively. We remeasured the reference stars from Greco et al. (2005) from the LOT *R*-band images and obtained the average magnitudes and rms errors.

[11] The errors in this article were quoted for a 68% (1 σ) confidence level.

TABLE 1
GRB 050319 OPTICAL AFTERGLOW PHOTOMETRY

Days after GRB[a]	Filter	Magnitude[b]	Site
0.05443	*R*	19.01 ± 0.08	Kiso
0.06023	*B*	20.42 ± 0.13	Kiso
0.08037	*V*	19.75 ± 0.07	Lulin
0.10439	*I*	19.09 ± 0.07	Lulin
0.27821	*B*	20.92 ± 0.12	Kiso
0.33424	*I*	19.91 ± 0.09	Lulin
0.40097	*V*	20.68 ± 0.12	Lulin
0.41346	*R*	20.20 ± 0.07	Lulin

NOTE.—Table 1 is published in its entirety in the electronic edition of the *Astrophysical Journal*. A portion is shown here for guidance regarding its form and content.

[a] The burst time is 2005 March 19, UT 09:29:01.44.

[b] The magnitudes are not corrected for Galactic extinction.

After fitting the *B*-, *V*-, *R*-, and *I*-band light curves to a single–power-law expression $F \propto t^{\alpha}$, where α is the index and t is the time after the burst, we get $\alpha = -0.56 \pm 0.06$ ($\chi^2/\nu = 2.90$ for $\nu = 19$) for the *B* band, $\alpha = -0.65 \pm 0.03$ ($\chi^2/\nu = 2.60$ for $\nu = 27$) for the *V* band, $\alpha = -0.59 \pm 0.01$ ($\chi^2/\nu = 5.3$ for $\nu = 97$) for the *R* band, and $\alpha = -0.52 \pm 0.15$ ($\chi^2/\nu = 7.7$ for $\nu = 9$) for the *I* band. This single–power-law fitting indicates that these light curves, obtained with different filters, have a similar power-law decay even though the reduced χ^2 values are relatively large.

Since the data sets of the *V* and *R* measurements are more complete, it is possible with following expression to attempt the fitting of the corresponding light curves with a smoothly broken power-law function:

$$F(\nu, t) = \frac{2^{1/k} F_{\nu, b}}{[(t/t_b)^{-k\alpha_1} + (t/t_b)^{-k\alpha_2}]^{(1/k)}}, \quad (1)$$

where t_b is the break time, α_1 and α_2 are the power-law indices before and after t_b, $F_{\nu, b}$ is flux at break t_b, and k is a smoothness factor. For the *V* band, we obtain $\alpha_1 = -0.87 \pm 0.21$, $\alpha_2 = -0.49 \pm 0.05$, $t_b = 0.042 \pm 0.058$ days, and $k = -30$ ($\chi^2/\nu = 1.48$ for $\nu = 24$). For the *R* band, we obtain $\alpha_1 = -0.84 \pm 0.02$, $\alpha_2 = -0.48 \pm 0.03$, $t_b = 0.046 \pm 0.008$ days, and $k = -21$ ($\chi^2/\nu = 2.24$ for $\nu = 90$). This result implies a mild break in both the *V*- and *R*-band light curves at around 0.04 days after the occurrence of the GRB.

Taking $t_b = 0.04$ days, we fit the data in the *B* and *I* bands to a respective power law before and after the break. In this manner, we find $\alpha_1 = -0.79 \pm 0.09$ ($\chi^2/\nu = 1.09$ for $\nu = 7$); $\alpha_2 = -0.36 \pm 0.05$ ($\chi^2/\nu = 1.23$ for $\nu = 9$) for the *B* band, and $\alpha_2 = -0.52 \pm 0.15$ ($\chi^2/\nu = 7.7$ for $\nu = 9$) for the *I* band. The best-fit parameters for the *B*, *V*, *R*, and *I* bands are summarized in Table 2. Our results show not only the clear presence of mild breaks in the *V*- and *R*-band light curves but a flattening trend after the break. Furthermore, our *R*-band slope before the break ($\alpha \sim -0.84$) is in agreement with the corresponding value derived by Quimby et al. (2006) for the interval between 0.0019 and 0.05 days after the burst.

3.2. *Color and Spectral Flux Distribution*

Our multiwavelength observations indicate that median colors between 0.07 and 0.35 days are $V - R = 0.45 \pm 0.11$, $R -$

TABLE 2
FITTING RESULTS OF THE GRB 050319 LIGHT CURVES

Filter	α_1	α_2	t_b (days)
B	-0.79 ± 0.09	-0.36 ± 0.05	...
V	-0.87 ± 0.21	-0.49 ± 0.05	0.042 ± 0.058
R	-0.84 ± 0.02	-0.48 ± 0.03	0.046 ± 0.008
I	...	-0.52 ± 0.15	...

NOTE.—The *B*- and *I*-band data were fitted by a respective power-law model ($F \propto t^{\alpha}$) before and after the break ($t_b = 0.04$ days). On the other hand, the *V* and *R* data were fitted by a smoothly broken power law (eq. [1]).

$I = 0.46 \pm 0.10$, and $B - V = 0.84 \pm 0.14$. These values have been corrected for foreground reddening of $E(B - V) = 0.011$ mag (Schlegel et al. 1998). The $V - R$ and $R - I$ colors so derived are consistent with those of the typical long GRBs (Simon et al. 2001), but the $B - V$ color is slightly redder than those of the typical long GRBs ($B - V = 0.47 \pm 0.17$). The larger $B - V$ value may imply a certain absorption effect because the redshift of GRB 050319 was determined to be 3.24 (Jakobsson et al. 2006).

The *B*, *V*, *R*, and *I* magnitudes have been further converted to fluxes using the effective wavelengths and normalizations of Fukugita et al. (1995). The effect of the Galactic interstellar extinction has been corrected. Figure 2 shows two samples of spectral energy distribution obtained by LOT 0.13 and 0.21 days after the occurrence of GRB 050319. A drop in the *B*-band flux at about 4380 Å can be clearly seen. We subsequently fitted the flux distribution of *V*, *R*, and *I* bands with a power-law function $F(\nu, t) \propto \nu^{\beta}$; here $F(\nu, t)$ is the flux at frequency ν with a certain t and β is the spectral index. We find that $\beta = -1.08 \pm 0.05$ ($\chi^2/\nu = 0.05$ for $\nu = 1$) at 0.13 days and that $\beta = -1.08 \pm 0.32$ ($\chi^2/\nu = 2.3$ for $\nu = 1$) at 0.21 days. Our result ($\beta = -1.08$ with an rms error of 0.23) is consistent with the X-ray fitting value ($\beta = -0.69 \pm 0.06$) in a 3 σ level.

With a redshift of 3.24, the Lyα absorption feature would shift into the *B* bandpass, causing reduction of the afterglow flux in the *B* band. To correct for this absorption effect, we used the formulation derived by Yoshii & Peterson (1994), in which the optical depth is a function of the observed wavelength and source redshift. With the computed optical depth in the *B* band, and a spectral slope of $\beta = -1.08$, we found the expected *B*-band magnitude after Lyα absorption to be 21.33 ± 0.05 at 0.13 days. This value compares very well with our observed value of $B = 21.26 \pm 0.17$ at 0.13 days after correction for Galactic extinction. The drop at the *B* band is hence fully produced by the Lyα absorption, and no spectral breaks should have taken place during our observation.

4. DISCUSSION AND SUMMARY

It is important to note that *Swift* found two breaks 0.004 and 0.313 days after the burst in the X-ray afterglow observations (Cusumano et al. 2006), but we only found a single break in our *V* and *R* light curves (see Fig. 1). In the following, since there are more data points available for the *R*-band data, we will focus on this. It is useful to remember that $\alpha_1 = -0.84$ and $\alpha_2 = -0.48$ at the break time of $t_b = 0.04$ days.

4.1. *Before the Optical Break* ($t < 0.04$ days)

The slope α_1 ($= -0.84$) is consistent with the typical range of $\alpha = -0.62$ to -2.3 for many well-observed GRBs. According to the standard afterglow model relating the power-law index (α) to the power-law index (p) of an electron spectrum (Zhang & Mészáros 2004; Dai & Cheng 2001), the

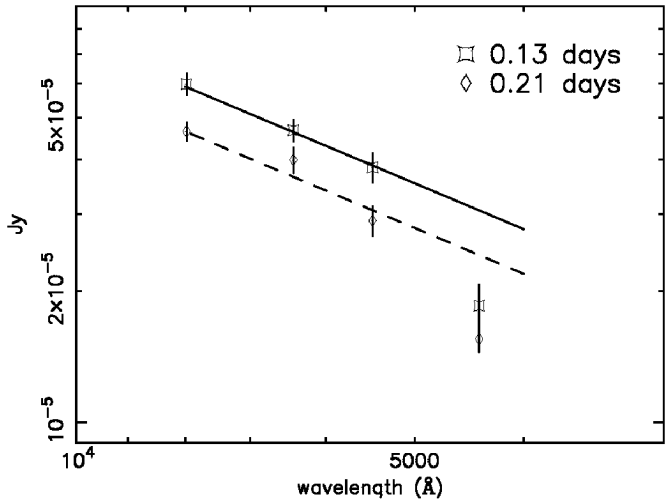

FIG. 2.—Spectral energy distribution of GRB 050319 between the *V*, *R*, and *I* bands 0.13 and 0.21 days after the burst (corrected for Galactic extinction). The solid and dashed lines indicate the best fit by the power-law model [$F(\nu) \propto \nu^{\beta}$], where $\beta = -1.08 \pm 0.05$ for 0.13 days and $\beta = -1.08 \pm 0.32$ for 0.21 days.

corresponding value for $\alpha_1 = -0.84$ is $p = 2.1$, which is in agreement with the constant-density ISM model with slow cooling in which $p > 2$ for $\nu_m < \nu_{\rm opt} < \nu_c$ (ν_m is the typical frequency; $\nu_{\rm opt}$ is the optical frequency; and ν_c is the cooling frequency). In light of the XRT observations, the first break was likely caused by the transition from the tail end of the low-energy prompt emission to the afterglow phase (Zhang et al. 2006). However, it is important to note that the X-ray break at 0.004 days (where the steeper slope becomes shallow) is not accompanied by an *R*-band break. At the same time, the power-law decay slope in the X-ray (~ -5.53) and that in the *R* band (~ -0.84) are quite different. This is an indication that the behaviors of the X-ray afterglow and optical afterglow of the GRB 050319 event are different, but this also suggests that the afterglow phase already dominated the optical bands when the optical emission was first detected.

4.2. *Shallow Decay*

The power-law index becomes shallow after the break ($t_b = 0.04$ days). Neither the jet (Rhoads 1999) nor the break frequencies across the optical wavelength (Sari et al. 1998) suitably explain the break we see in the GRB 050319 light curves. As discussed before, the X-ray light curve between the two breaks 0.004 and 0.313 days after the burst is also characterized by shallow decay. Several studies indicate that such behavior is related to continuous energy injection into the ISM (Dai & Lu 1998a, 1998b; Zhang et al. 2006). For a long-lasting central engine, the energy injection rate is $E(t) \propto t^{-q}$, with $q < 1$ (Zhang & Mészáros 2001). For slow cooling in the ISM, the temporal index can be expressed as $\alpha = [(2p - 6) + (p + 3)q]/4 = [(q - 1) + (2 + q)\beta]/2$, when $\nu_m < \nu < \nu_c$. Using this formulation, Zhang et al. (2006) obtained $q = 0.6$ and $p = 2.4$ from the X-ray observations. With $\alpha = -0.48$ and $\beta = -1.08$ from the *R*-band observations, we find that $q = 0.72$ and $p = 2.12$. The results not only indicate that the electron spectrum power-law index is the same before and after the break, but they also compare well with the results of Zhang et al. (2006). These results indicate that the shallow decays evidenced by both X-ray and optical afterglows could be of a similar origin, related to a continuous energy injection mechanism.

According to the energy injection model, we would also

expect an X-ray break at the time of the optical flattening break, because the onset of the energy injection should also alter the X-ray temporal index. However, such an X-ray break is not observed, which suggests that some modifications to the injection model may be needed. As mentioned in § 4.1, the X-ray break at 0.004 days was not accompanied by a break in the *R* light curve. Although a chromatic break in the X-ray was found at 0.004 days and in the optical region at 0.04 days, the light curves at both wavelengths indeed showed shallow decay after the breaks, which can be explained by the energy injection model. However, it is difficult for energy injection from 0.004 to 0.04 days to affect only high energies. This difficulty indicates that energy injection is an imperfect mechanism for explaining the shallow optical or X-ray phase associated with the GRB 050319 event.

Several models have recently been proposed to explain the shallow decay effect. Using the multiple-subjet model (Nakamura 2000), Toma et al. (2006) invoked the superposition of afterglows from many off-axis subjets. Eichler & Granot (2006) favored a combination of the tail of prompt emission model with the afterglow emissions observed from a viewing angle outside the edge of the jet. These arguments hence suggest that the multiple-subjet model and the patchy-shell model (Kumar & Piran 2000) might provide a theoretical basis for explaining the observed shallow decays in the X-ray and optical light curves. It is interesting to note that in order to sustain the shallow decay process, these models all require high gamma-ray efficiency (75%–90%); additional mechanisms such as prior activity (Ioka et al. 2006) and time-dependent shock generation (Fan & Piran 2006) have also been proposed. Comprehensive multiwavelength observations, such as those reported here, provide us with important ways to improve these models.

Finally, the second break in the X-ray emissions (~0.313 days) has been interpreted as being due to an unusual flat jet break (Cusumano et al. 2006); however, Zhang et al. (2006) provided an alternate explanation, a sudden cessation of the energy injection. In both interpretations, the corresponding break should appear in both the X-ray and optical light curves. This effect cannot be clearly identified in our measurements until 0.413 days after the burst. The lack of data for the subsequent time interval could lead to uncertainty in the power-law fitting. We thus cannot fully exclude the existence of a second break in the optical light curves. However, Panaitescu et al. (2006) have studied several afterglows. They found the shallow power-law decay evidenced by the X-ray emissions to steepen about 0.04–0.17 days after the burst, although there was no accompanying break found in the optical range. They suggest that such chromatic X-ray breaks may be common. The chromatic breaks (e.g., the shallow X-ray phase becomes steeper, with no accompanying optical break) may be caused by differences in the X-ray and optical outflow (Panaitescu et al. 2006) or by changes in the typical electron energy parameters (the so-called microphysical parameters) at the end of energy injection (Panaitescu 2006).

In summary, our analysis of the optical multiwavelength observations of GRB 050319 compared with the X-ray observations from *Swift* found the following major results:

1. The *B*, *V*, *R*, and *I* band light curves displayed unusual shallow decays.
2. The *R* light curve can be described by a smooth broken power-law function; $\alpha_1 \sim -0.84$ becomes shallow ($\alpha_2 \sim -0.48$) 0.04 days after the occurrence of the GRB.
3. The shallow decay observed in the X-ray and optical light curves may have a similar origin related to energy injection. However, our observations indicate that a major puzzle remains concerning the chromatic breaks in the *R*-band light curve (at 0.04 days) and the X-ray light curve (at 0.004 days).
4. Our calculations revealed that the drop in spectral energy distribution was fully caused by a shift in the Lyα absorption to the *B* bandpass at $z = 3.24$.

We thank the referee for his/her valuable advice. This work is supported by NSC 95-2752-M-008-001-PAE, NSC 95-2112-M-008-021, the Japan Society for the Promotion of Science (JSPS) Grant-in-Aid for Young Scientists (B) 18740147, and JSPS Research Fellowships for Young Scientists (Y. U.).

REFERENCES

Blustin, E., et al. 2006, ApJ, 637, 901
Cusumano, G., et al. 2006, ApJ, 639, 316
Dai, Z. G., & Cheng, K. S. 2001, ApJ, 558, L109
Dai, Z. G., & Lu, T. 1998a, A&A, 333, L87
———. 1998b, Phys. Rev. Lett., 81, 4301
Eichler, D., & Granot, J. 2006, ApJ, 641, L5
Fan, Y., & Piran, T. 2006, MNRAS, 369, 197
Fukugita, M., Shimasaku, K., & Ichikawa, T. 1995, PASP, 107, 945
Gehrels, N., et al. 2004, ApJ, 611, 1005
George, K., Banerjee, D. P. K., Chandrasekhar, T., & Ashok, N. M. 2006, ApJ, 640, L13
Greco, G., Bartolini, C., Guarnieri, A., Piccioni, A., Ferrero, P., & Bruni, I. 2005, GCN Circ. 3142, http://gcn.gsfc.nasa.gov/gcn/gcn3/3142.gcn3
Henden, A. 2005, GCN Circ. 3454, http://gcn.gsfc.nasa.gov/gcn/gcn3/3454.gcn3
Ioka, K., Toma, K., Yamazaki, R., & Nakamura, T. 2006, A&A, 458, 7
Jakobsson, P., et al. 2006, A&A, 460, L13
Kinoshita, D., Chen, C.-W., Lin, H.-C., Lin, Z.-Y., Huang, K.-Y., Chang, Y.-S., & Chen, W.-P. 2005, Chinese J. Astron. Astrophys., 5, 315
Kiziloglu, U., et al. 2005, GCN Circ. 3139, http://gcn.gsfc.nasa.gov/gcn/gcn3/3139.gcn3
Krimm, H., et al. 2005, GCN Circ. 3119, http://gcn.gsfc.nasa.gov/gcn/gcn3/3119.gcn3
Kumar, P., & Piran, T. 2000, ApJ, 535, 152
Mason, K. O., et al. 2006, ApJ, 639, 311
Misra, K., Kamble, A. P., & Pandey, S. B. 2005, GCN Circ. 3130, http://gcn.gsfc.nasa.gov/gcn/gcn3/3130.gcn3
Nakamura, T. 2000, ApJ, 534, L159
Nousek, J. A., et al. 2006, ApJ, 642, 389
Panaitescu, A. 2006, preprint (astro-ph/0607396)
Panaitescu, A., Mészáros, P., Burrows, D., Nousek, J., O'Brien, P., & Willingale, R. 2006, MNRAS, 369, 2059
Quimby, R. M., et al. 2006, ApJ, 640, 402
Rhoads, J. E. 1999, ApJ, 525, 737
Rykoff, E., et al. 2006, ApJ, 638, L5
Sari, R., Piran, T., & Narayan, R. 1998, ApJ, 497, L17
Schlegel, D. J., Finkbeiner, D. P., & Davis, M. 1998, ApJ, 500, 525
Sharapov, D., et al. 2005a, GCN Circ. 3124, http://gcn.gsfc.nasa.gov/gcn/gcn3/3124.gcn3
———. 2005b, GCN Circ. 3140, http://gcn.gsfc.nasa.gov/gcn/gcn3/3140.gcn3
Simon, V., Hudec, R., Pizzichini, G., & Masetti, N. 2001, A&A, 377, 450
Stetson, P. B. 1987, PASP, 99, 191
Toma, K., Ioka, K., Yamazaki, R., & Nakamura, T. 2006, ApJ, 640, L139
Torii, K. 2005, GCN Circ. 3121, http://gcn.gsfc.nasa.gov/gcn/gcn3/3121.gcn3
Urata, Y., et al. 2005, Nuovo Cimento, 28, 775
Woźniak, P. R., Vestrand, W. T., Wren, J. A., White, R. R., Evans, S. M., & Casperson, D. 2005, ApJ, 627, L13
Yoshii, Y., & Peterson, B. A. 1994, ApJ, 436, 551
Yoshioka, T., et al. 2005, GCN Circ. 3120, http://gcn.gsfc.nasa.gov/gcn/gcn3/3120.gcn3
Zhang, B., & Mészáros, P. 2001, ApJ, 552, L35
———. 2004, Int. J. Mod. Phys. A, 19, 2385
Zhang, B., et al. 2006, ApJ, 642, 354